

The giant arc statistics in the three year WMAP cosmological model

G. L. Li^{1,2*}, S. Mao³, Y.P. Jing^{1,2}, H.J. Mo⁴, L. Gao⁵, W.P. Lin^{1,2}

¹ Shanghai Astronomical Observatory, Nandan Road 80, Shanghai 200030, China

² Joint Institute for Galaxy and Cosmology (JOINGC) of SHAO and USTC

³ University of Manchester, Jodrell Bank Observatory, Macclesfield, Cheshire SK11 9DL, U.K.

⁴ Department of Astronomy, University of Massachusetts, Amherst MA 01003-9305, USA

⁵ Institute for Computational Cosmology, Physics Department, Durham, DH1 3LE, U.K.

Accepted 2006 August 7. Received 2006 August 4; in original form 2006 July 5

ABSTRACT

We use high-resolution N -body simulations to investigate the optical depth of giant arcs with length-to-width ratio larger than 7.5 and 10 in the ‘standard’ Λ CDM model with $\sigma_8 = 0.9$ and $\Omega_{m,0} = 0.3$ and a model based on three-year Wilkinson Microwave Anisotropy Probe (WMAP) data. We find that, in dark-matter only simulations, the lensing probability in the three-year WMAP model (with $\sigma_8 = 0.74$ and $\Omega_{m,0} = 0.238$) decreases by a factor of ~ 6 compared with that in the ‘standard’ Λ CDM model. The effects of baryonic cooling, star formation and feedbacks are uncertain, but we argue that baryons will only increase the the lensing cross-section by a moderate factor, ~ 2 . We conclude that the low central value of σ_8 and $\Omega_{m,0}$ preferred by the WMAP three-year data may be too low to be compatible with observations if conventional assumptions of the background source population are correct.

Key words: cosmology: galaxy clusters – gravitational lensing

1 INTRODUCTION

In the hierarchical scenario of structure formation, structures in the universe are assumed to have grown from tiny quantum fluctuations generated during an inflation period through gravitational instability. Inflationary models predict that the initial fluctuations are Gaussian and have a roughly scale-free power-spectrum: $P(k) \propto k^n$ with $n \sim 1$. The amplitude of the power spectrum, for which a reliable prediction from inflationary theory is still lacking, has to be determined from observations. This amplitude is usually represented by a quantity, σ_8 , which is the *RMS* of the linear density perturbations within a spherical window of radius $8h^{-1}$ Mpc, where h the Hubble constant in units of $100 \text{ km s}^{-1} \text{ Mpc}^{-1}$.

The linear power spectrum can be probed with a variety of observations, ranging from abundances of clusters, weak gravitational lensing, large-scale structure in galaxy distribution, galaxy motions, Lyman- α forests, and most importantly, the temperature fluctuations in the cosmic microwave background (see Spergel et al. 2006, and references therein). Recent results from the three-year data of the Wilkinson Microwave Anisotropy Probe (WMAP) alone prefers a σ_8 value of $0.74^{+0.06}_{-0.05}$. Although the errorbar is still quite large, the median value is lower than the value, $\sigma_8 = 0.9$, adopted

in the ‘standard’ Λ CDM model. The lower value of σ_8 is favored by a number of other observations related to the clustering of galaxies (e.g. Jing, Mo & Börner 1998; Yang et al. 2004, 2005; van den Bosch, Mo & Yang 2003; Tinker et al. 2006; Sánchez et al. 2006), but weak lensing results (e.g. Bacon et al. 2004; Van Waerbeke et al. 2002) and data on Lyman alpha forests (Viel, Haehnelt & Lewis 2006; Seljak, Slosar & McDonald 2006) seem to prefer a higher value.

As the largest bound structures in the universe, clusters of galaxies provide a sensitive probe for σ_8 , because their abundance in the universe depends sensitively on the amplitude of the density perturbations (and also the matter content in the universe, $\Omega_{m,0}$). The abundance of clusters can be determined from X-ray (e.g. Rosati et al. 2002; Popesso et al. 2004; Reiprich & Böhringer 2002; Reiprich 2006) and optical surveys (e.g. Gladders et al. 2006). However, in order to use the observed abundance to constrain model of structure formation, one has to know the masses of these objects accurately. This is in general difficult to do. For example, X-ray studies usually assume hydrostatic equilibrium in order to derive the cluster mass, which may be invalid for many (such as merging) clusters (e.g. Gao & White 2006). Another probe of the abundance of clusters is giant arcs that are produced when background galaxies are tangentially stretched by foreground clusters (e.g. Luppino et al. 1999; Zaritsky & Gonzalez 2003;

* E-mail: lg1@shao.ac.cn

Table 1. Cosmological simulation parameters. The columns are cosmology, box size, number and mass of dark matter particles, and the softening length.

model	box size (h^{-1} Mpc)	N_{DM}	m_{DM} ($h^{-1}M_{\odot}$)	softening (h^{-1} kpc)
Λ CDM0	300	512^3	1.67×10^{10}	30
WMAP3	300	512^3	1.32×10^{10}	30

Gladders et al. 2003; Sand et al. 2005). A number of recent investigations made comparisons between the observed abundance of giant arcs with that expected in the ‘standard’ Λ CDM model with $\sigma_8 = 0.9$ (Dalal et al. 2004; Li et al. 2005; Hennawi et al. 2005; Horesh et al. 2005), finding agreement between model and observation (Dalal et al. 2004; Wambsgans et al. 2004). In light of the change in cosmological parameters preferred by the WMAP three-year data, it becomes important to re-evaluate how the predicted lensing probability changes.

In this paper, we study the number of giant arcs expected in the new cosmological model, using high resolution N -body simulations. We compare the results with those obtained from similar simulations of the standard Λ CDM model, and with current observations. The plan of the paper is as follows. In §2, we describe the simulations we use and the analysis to predict giant arcs in the N -body simulations. Our main results are presented in §3, and we finish with a discussion in §4.

2 COSMOLOGICAL MODELS, NUMERICAL SIMULATIONS, AND LENSING METHOD

In this paper, we use two sets of simulations, one for the ‘standard’ Λ CDM model with $\sigma_8 = 0.9$, and the other for the cosmological model given by the recent three-year WMAP data with $\sigma_8 = 0.74$. For brevity, these two models will be referred to as Λ CDM0, and WMAP3, respectively, and the corresponding cosmological parameters are:

- (i) Λ CDM0: $\Omega_{\text{m},0} = 0.3, \Omega_{\Lambda,0} = 0.7, h = 0.7, \sigma_8 = 0.9, n = 1$;
- (ii) WMAP3: $\Omega_{\text{m},0} = 0.238, \Omega_{\Lambda,0} = 0.762, h = 0.73, \sigma_8 = 0.74, n = 0.95$.

The assumed initial transfer function in each model was generated with CMBFAST (Seljak & Zaldarriaga 1996). Notice that both σ_8 and $\Omega_{\text{m},0}$ differ in these two models.

We use a vectorized-parallel P³M code (Jing & Suto 2002) and a PM-TREE code – GADGET2 (Springel, Yoshida, White 2001; Springel 2005) to simulate the structure formation in these models; the details of the simulations are given in Table 1. Both are N -body simulations which evolve $N_{\text{DM}} = 512^3$ dark matter particles in a large cubic box with sidelength equal to $300h^{-1}$ Mpc. The Λ CDM0 simulation was performed using the P³M code of Jing & Suto (2002) and has been used in Li et al. (2005) to study the properties of giant arcs. We refer the readers to that paper for the detail. The WMAP3 simulation is a new simulation carried out with GADGET2. With their large volumes, these two simulations sample the corresponding cluster mass functions reasonably well, and they will be

used to compare the optical depths of giant arcs in the Λ CDM0 and WMAP3 models.

For each simulation, we identify virialised dark matter halos using the friends-of-friends method with a linking length equal to 0.2 times the mean particle separation. The halo mass M is defined as the virial mass within the virial radius according to the spherical collapse model (Kitayama & Suto 1996; Bryan & Norman 1998; Jing & Suto 2002). Giant arcs are produced mainly by clusters of galaxies, and so we focus on massive haloes with $M \gtrsim 10^{14}h^{-1}M_{\odot}$.

For a given cluster, we calculate the smoothed surface density maps using the method of Li et al. (2006). Specifically, for any line of sight, we obtain the surface density on a 1024×1024 grid covering a square of (comoving) sidelength of $4h^{-1}$ Mpc centered on each cluster. The projection depth is chosen to be $4h^{-1}$ Mpc. Particles outside this cube and large-scale structures do not contribute significantly to the lensing cross-section (e.g. Li et al. 2005; Hennawi et al. 2005). Our projection and smoothing method uses a smoothed particle hydrodynamics (SPH) kernel to distribute the particle mass on a 3D grid and then integrate along the line of sight to obtain the surface density (see Li et al. 2006 for detail). In this work, the number of neighbors used in the SPH smoothing kernel is fixed to be 32. Once a surface density map is obtained, we compute the cross-section of giant arc formation following the method given in Li et al. (2005). We consider seven source redshifts, $z_s = 0.6, 1.0, 1.5, 2.0, 3.0, 4.0$ and 7.0 . The background sources are assumed to be elliptical with random position angles and a fixed angular surface area, $S_{\text{source}} = \pi \times 0.5''^2$. The axis ratio is randomly drawn between 0.5 and 1. This choice of axis ratio and source size is in good agreement with the study of high-redshift galaxies using HST by Ferguson et al. (2004). We generate a large number of background sources within a rectangle box with area S_{box} . This rectangle is chosen to enclose all the high-magnification regions that can potentially form giant arcs. The number of sources generated is given by $n_{\text{source}} = 9S_{\text{box}}/S_{\text{source}}$. For each source, ray-tracing is used to find the resulting image(s). Giant arcs are identified as elongated images with length-to-width (L/W) ratio exceeding 7.5 or 10, the usual criterion used to select giant arcs in observations. We calculate the total cross sections of the top 200 most massive clusters in each simulation output and obtain the average cross section per unit comoving volume by:

$$\bar{\sigma}(z_1, z_s) = \frac{\sum \sigma_i(z_1, z_s)}{V}, \quad (1)$$

where $\sigma_i(z_1, z_s)$ is the average cross-section of the three projections of the i -th cluster at redshift z_1 , z_s is the source redshift, and V is the comoving volume of the simulation box. The optical depth can then be calculated as:

$$\tau(z_s) = \frac{1}{4\pi D_s^2} \int_0^{z_s} dz \bar{\sigma}(z, z_s) (1+z)^3 \frac{dV_p(z)}{dz}, \quad (2)$$

where D_s is the angular diameter distance to the source, and $dV_p(z)$ is the proper volume of a spherical shell with redshift from z to $z + dz$. The integration step size is the same as the redshift interval of simulation output ($dz \approx 0.1$).

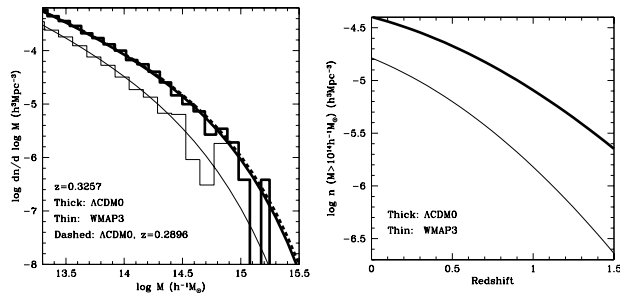


Figure 1. The left panel shows the number density of halos in the Λ CDM0 (thick) and WMAP3 (thin) cosmological models (see text) at redshift 0.33 obtained using the Sheth-Tormen mass function (2002). The thin solid histogram shows the number density of haloes found in a simulation with box size $300h^{-1}$ Mpc in the WMAP3 model at $z = 0.33$. The thick solid histogram shows the number density of haloes in the Λ CDM0 simulation at $z = 0.2896$ (the corresponding theoretical prediction is shown as the thick dashed line). The right panel shows how the number density of haloes with mass $M > 10^{14} h^{-1} M_\odot$ evolves as a function of redshift in the two cosmologies.

3 RESULTS

The left panel of Fig. 1 shows the mass functions in the two cosmological models at redshift 0.3, the optimal lensing redshift for a source at redshift 1 (see the right panel of Fig. 2). The mass functions are calculated following Sheth & Tormen (2002), which is based on the Press-Schechter (1974) formalism and the ellipsoidal collapse model (Sheth, Mo & Tormen 2001). The mass functions (shown as histograms) in simulations clearly match the predictions well. We can see that the number density of haloes in the WMAP3 model is always smaller than that in the Λ CDM0 model on cluster mass scale. For $M \sim 10^{14} h^{-1} M_\odot$, the abundance of haloes is lower by a factor of 2.6 in the WMAP3 model compared with that in the Λ CDM0 model; for $M \sim 10^{15} h^{-1} M_\odot$, the reduction factor is ~ 8.3 . The lower abundance of clusters in the WMAP3 model implies that ideally a larger simulation box is required to sample a similar number of massive clusters as in the Λ CDM0 model, a point we return to briefly in the discussion.

The right panel in Fig. 1 shows how the predicted number density of haloes above $10^{14} h^{-1} M_\odot$ evolves as a function of redshift in these two cosmologies. The ratio of the number density of massive haloes in the WMAP3 model and that in the Λ CDM0 model as a function of redshift is well approximated (within 10%) by $0.4 - 0.2z$ for $z < 1.5$. At redshift 0.3, 0.5 and 1, the number density of haloes above $10^{14} h^{-1} M_\odot$ is about 1/3, 1/5 and 1/10 of that in the Λ CDM0 respectively. Notice that the cosmological distances and volumes also differ in the three models, but the differences (which are accounted for in our calculations) are small, ranging from 11% for the angular diameter distances and 6% for the volume out to a source redshift of 2. These differences are much smaller than the change in the cluster abundance.

As a consequence of the lower cluster abundance in the WMAP3 model, one expects the lensing optical depth will also be much lower compared with that in the Λ CDM0 model. This is illustrated in the left panel of Fig. 2 which shows the optical depths as a function of the source redshift

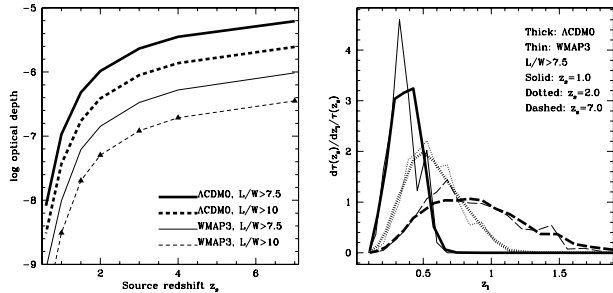


Figure 2. The left panel shows the optical depth as a function of source redshift in the Λ CDM0 and WMAP3 models for giant arcs with $L/W > 7.5$ and $L/W > 10$. The right panel shows the differential probability distribution for the optical depth as a function of lens redshift for $z_s = 1, 2$ and 7 respectively. In both panels, the results for the Λ CDM0 and WMAP3 models are shown as thick and thin curves respectively.

in the Λ CDM0 and WMAP3 models. First, we notice that the optical depth is a strong function of the source redshift, z_s , particularly when $z_s < 3$, a trend first emphasized by Wambsganss et al. (2004). Second, it is clear that the optical depth in the WMAP3 model is much lower: compared with that in the Λ CDM0 model, the optical depth is reduced by more than a factor of ~ 6 for $L/W > 7.5$ and 10 at all source redshifts. The right panel of Fig. 2 shows the differential probability distribution of the optical depth for giant arcs with $L/W > 7.5$ as a function of the lens redshift for $z_s = 1, 2$, and 7 ; the trends (not shown) are similar for $L/W > 10$. For a source at redshift 1, 2 and 7, the optimal lensing redshift is around 0.3, 0.5 and 0.75, respectively, in the two cosmologies considered here. Note that the normalised shapes are quite similar in the two cosmological models but the overall optical depth is much lower in the WMAP3 model.

4 DISCUSSIONS

We have compared, using high-resolution N -body simulations, the lensing probabilities of giant arcs in two cosmological models: the old ‘concordance’ model with $\sigma_8 = 0.9$, and the model with parameters given by the three-year WMAP data. We find that the lensing probability decreases by a factor of ~ 6 in the 3-year WMAP model compared to that in the Λ CDM0 concordance model. This decrease is largely a result of the much lower number density of massive haloes in the WMAP3 model (see Fig. 1).

There has been a long debate whether the number of observed giant arcs is consistent with theoretical predictions. Early comparisons use simple analytical models (Kormann et al. 1994; Wu & Hammer 1993; Wu & Mao 1996; see also Oguri et al. 2003), which were later shown to severely under-estimate the lensing optical depth (Bartelmann & Weiss 1994; Bartelmann, Steinmetz & Weiss 1995; Meneghetti et al. 2003a; Torri et al. 2004). Many recent studies use N -body simulations, but with only dark matter (e.g. Wambsganss et al. 2004; Dalal et al. 2004, see Puchwein et al. 2005 for an exception). Below we discuss the uncertainties in both observations and predictions, and ex-

amine the consistency found in several previous works in the Λ CDM0 cosmology.

4.1 Consistency in the Λ CDM0 cosmology

Several previous studies concluded that the observational results of giant arcs are compatible with theoretical predictions (Oguri et al. 2003; Wambsganss et al. 2004; Dalal et al. 2004) in the Λ CDM0 cosmology. However, there are uncertainties in such conclusion.

The study by Oguri et al. (2003) used the axis ratio distributions in the tri-axial model of Jing & Suto (2002), and assumed a central profile, $\rho \propto r^{-1.5}$, that are steeper than the Navarro, Frenk & White (1997) form. Gas cooling can steepen the halo density profile, but it also makes the central mass distribution rounder. In this case, the shape distributions obtained in dark matter-only simulations are not suitable for clusters where gas cooling steepens the density profile dramatically. Since a shallower profile or a more spherical shape will reduce the giant arc cross-sections, it is unclear whether or not the conclusion of Oguri et al. (2003) still holds if consistent models for density profile and halo shape are used. Wambsganss et al. (2004) assumes that the L/W ratio can be approximated by the magnification. This assumption is valid for isothermal spheres, but not for real clusters which appear to be well fit by the Navarro, Frenk & White (1997) profile (van de Marel et al. 2000; Comerford et al. 2006; Voigt & Fabian 2006). This assumption over-estimates the optical depth by a factor of few (Dalal et al. 2004; Li et al. 2005). Furthermore, they also assumed a slightly higher normalization, $\sigma_8(0.95)$, which also increases the optical depth. The study by Dalal et al. (2004) assumes that arcs can be approximated as rectangles, which may overestimate the total cross-section by a factor of two compared to the perhaps more realistic assumption of elliptical arcs. In summary, even in the Λ CDM0 cosmology, the consistency between observations and predictions requires somewhat optimistic assumptions. The WMAP3 model, which predicts an optical depth by a factor of ~ 6 smaller, makes it even harder to explain the observed giant arcs.

4.2 Effects of baryons

In the real universe, baryons account for roughly 20% of the total mass, which can cool (form stars) and sink toward the centres of clusters. The radiative cooling likely has two effects: it will increase the concentration of baryons at the center of clusters, and at the same time, make the clusters more spherical (e.g. Dubinski 1994; Kazantzidis et al. 2004). The former increases while the latter decreases the lensing cross-sections, and so the overall influence depends on which effect dominates.

Puchwein et al. (2005) studied the lensing cross-sections of clusters with $M \gtrsim 10^{15} h^{-1} M_\odot$ with different prescriptions of numerical viscosities. They concluded that the higher concentrations due to baryons dominate and the baryons increase the lensing cross-sections by a factor of ~ 2 . However, they cautioned that their clusters may suffer from overcooling, as the stellar density in the core is larger than observed, and so the effect of baryons may be over-estimated. Notice

also that their simulations did not include feedbacks from active galactic nuclei, which may further decrease the cooling of baryons at cluster centres and the corresponding lensing cross-sections. As the star formation treatment in hydrodynamical simulations is uncertain, Meneghetti et al. (2003b) adopted an alternate empirical approach. They studied the effect of baryons by including a central cD galaxy in clusters. They found that the increase in the lensing cross-section due to cD galaxies is again quite moderate, by a factor of $\lesssim 2$. Such an enhancement cannot compensate the reduction in the optical depth due to the lower abundance of clusters in the WMAP3 model compared with the Λ CDM0 model.

4.3 Uncertainties in the cluster and background source populations

The cluster abundance (but not internal structures, particularly when star formation is included) can now be reliably predicted from both numerical simulations and the extended Press-Schechter analytic formalism. In the Λ CDM0 cosmology, various investigations, using similar assumptions of the background source population and definition of the length-to-width ratio, predict lensing optical depths that agree with one another within a factor of 1.5 (e.g. Dalal et al. 2004; Li et al. 2005; see Li et al. 2005 for a detailed discussion). We caution, however, that even our $300h^{-1}$ Mpc box size still appears to be somewhat too small to sample the tail of the cluster mass function well, as is shown by the large noise in the right panel of Fig. 2. We have 158 clusters with $M > 10^{14} h^{-1} M_\odot$ (7 clusters with $M > 3.8 \times 10^{14} h^{-1} M_\odot$). At redshift $z = 0.3$ for $z_s = 3$, 50% of the giant arc cross-section is contributed by clusters with $M > 3.8 \times 10^{14} h^{-1} M_\odot$. The larger noise may also be partly due to our inadequate sampling of merger events as we only dump the simulation data with a redshift interval of $dz \approx 0.1$. As shown by a number of previous works (Torri et al 2004; Hennawi et al. 2005; Fedeli et al. 2006), merger events can boost the lensing cross-sections significantly. To examine the importance of this effect, we ran a lower resolution simulation in the WMAP3 model which evolves $N_{\text{DM}} = 512^3$ dark matter particles in a box with sidelength of $600h^{-1}$ Mpc. Due to the larger volume, the new simulation better samples the high mass tail of the cluster mass function and merger events. The optical depth decreases by a factor of ~ 2 . The larger optical depth in our first WMAP3 simulation is partly because it has relatively more massive clusters than the larger simulation due to cosmic variance. Furthermore, the poorer resolution of the larger simulation may have also reduced the optical depth, and so the real change should be $\lesssim 2$.

Substructures along the line of sight may be important for the anomalous flux ratio problem (Metcalf 2005), but are unlikely to be important for the lensing cross-sections as they are expected to contribute only a few per cent of the surface density. Notice that we use a cube of $4h^{-1}$ Mpc to evaluate the lensing cross-sections. In Li et al. (2005) the sidelength is chosen to be $2r_{\text{vir}}$. These two choices give almost identical optical depths (compare Fig. 2 with Fig.7 in Li et al. 2005). This demonstrates that the influence of matter (including substructures) in the outer skirts of clusters is not important.

A much larger uncertainty concerns the background source population, including their ellipticity, size and red-

shift distributions. While the former two appear to have modest effects on the lensing cross-sections (e.g. Oguri 2002; Li et al. 2005), the source redshift distribution has quite dramatic effects on the lensing cross-section (Wambsganss et al. 2004), as can be seen in Fig. 2. This is the biggest uncertainty in the predictions of giant arcs. More redshift measurements of giant arcs will be particularly useful to clarify the situation (see Covone et al. 2006 for a recent effort).

Currently the giant arc samples are still small. The largest dedicated search for giant arcs in X-ray clusters was performed by Luppino et al. (1999) who found strong lensing in 8 out of 38 clusters. In the optical, Zaritsky & Gonzalez (2003) found two giant arcs using the Las Campanas Distant Cluster Survey between redshift 0.5 and 0.7 in an effective search area of 69 square degrees while Gladders et al. (2003) found eight clusters with giant arcs using the Red-Sequence Cluster Survey over ~ 90 square degrees. The largest arc sample found from HST archives was presented by Sand et al. (2005) with 116 arcs from 128 clusters, although its selection function is likely heterogeneous. Clearly the current giant arc samples are somewhat limited, although future weak lensing surveys (e.g. Wittman et al. 2006) may yield a large number of giant arcs as a by-product. A combined analysis of strong and weak lensing will be particularly useful for constraining σ_8 and the cluster inner mass profiles.

Until larger arc samples become available and our understanding of the background source population is improved, it is difficult to reach firm conclusions concerning the consistency of the WMAP three-year model with observations. Nevertheless, it appears difficult to reconcile the giant arc statistics with the low central σ_8 value (0.74) preferred by the WMAP three-year data.

ACKNOWLEDGMENT

We thank Volker Springel for providing the code GADGET2 and the referee for insightful comments. This work is supported by grants from NSFC (No. 10373012, 10533030) and Shanghai Key Projects in Basic research (No. 04JC14079 and 05XD14019). HJM, LG and SM acknowledge travel support from the Chinese Academy of Sciences. The simulations were performed at the Shanghai Supercomputer Center.

REFERENCES

- Bacon D. J., Massey R. J., Refregier A. R., Ellis R. S., 2003, MNRAS, 344, 673
- Bartelmann M., Weiss A., 1994, A&A, 287, 1
- Bartelmann M., Steinmetz M., Weiss A., 1995, A&A, 297, 1
- Bartelmann M., Meneghetti M., 2004, A&A, 418, 413
- Bryan G. L., Norman M. L. 1998, ApJ, 495, 80
- Comerford J. M., Meneghetti M., Bartelmann M., Schirmer M., 2006, ApJ, 642, 39
- Covone G., Kneib J.-P., Soucail G., Richard J., Jullo E., Ebeling H., 2006, A&A, submitted
- Dalal N., Holder G., Hennawi J.F., 2004, ApJ, 609, 50
- Dubinski J., 1994, ApJ, 431, 617
- Fedeli C., Meneghetti, M., Bartelmann M., Dolag K., Moscardini L., 2006, A&A, 447, 419
- Ferguson H. C., et al., 2004, ApJ, 600, L107
- Gao L., White S. D. M., 2006, MNRAS, submitted (astro-ph/0605087)
- Gladders M. D., Hoekstra H., Yee H. K. C., Hall Patrick B., Barrientos L. F., 2003, ApJ, 593, 48
- Gladders M. D., Yee H. K. C., Majumdar S., Barrientos L. F., Hoekstra, H., Hall, Patrick, B., Infante, L. 2006, preprint (astro-ph/0603588)
- Hennawi J. F., Dalal N., Bode P., Ostriker J. P., 2005, preprint (astro-ph/0506171)
- Hoesh A., Ofek E. O., Maoz D., Bartelmann M., Meneghetti M., Rix H.-W., 2005, ApJ, 633, 768
- Jing Y. P., Suto Y. 2002, ApJ, 574, 538
- Jing Y. P., Mo H. J., Börner G. 1998, ApJ, 494, 1
- Kazantzidis S., Kravtsov A. V., Zentner A. R., Allgood B., Nagai D., Moore B., 2004, ApJ, 611, L73
- Kitayama T., Suto Y., 1996, MNRAS, 280, 638
- Kormann R., Schneider P., Bartelmann M., 1994, AA, 284, 285
- Li G. L., Mao S., Jing Y. P., Bartelmann M., Kang X., Meneghetti M., 2005, ApJ, 635, 795
- Li G. L., Mao S., Jing Y. P., Kang X., Bartelmann M., 2006, ApJ, in press (astro-ph/0603557)
- Luppino G. A., Gioia I. M., Hammer F., Le Fèvre O., Annis J. A., 1999, AAS, 136, 117
- Metcalfe R. B., 2005, ApJ, 629, 673
- Meneghetti M., Bartelmann M., Moscardini L., 2003a, MNRAS, 340, 105
- Meneghetti M., Bartelmann M., Moscardini L., 2003b, MNRAS, 346, 67
- Navarro J. F., Frenk C. S., White S. D. M., 1997, ApJ, 490, 493
- Oguri M., Lee J., Suto Y., 2003, ApJ, 599, 7
- Oguri M., 2002, ApJ, 573, 51
- Popesso P., Böringer H., Brinkmann J., Voges W., York D. G., 2004, A&A, 423, 449
- Press W. H., Schechter P. L. 1974, ApJ, 187, 425
- Puchwein E., Bartelmann M., Dolag K., Meneghetti M., 2005, A&A, 442, 405
- Reiprich, T. H., 2006, astro-ph/0605009
- Reiprich T. H., Böringer H., 2002, ApJ, 567, 716
- Rosati P., Borgani S., Norman C., 2002, ARA&A, 40, 539
- Sánchez A. G. et al., 2006, MNRAS, 366, 189
- Sand D. J., True T., Ellis R. S., Smith G. P., 2005, ApJ, 627, 32
- Seljak U., Slosar A., McDonald P., 2006, astro-ph/0604335
- Seljak U., Zaldarriaga M., 1996, ApJ, 469, 437
- Sheth R. K., Tormen G., 2002, 329, 61
- Sheth R. K., Mo H. J., Tormen G., 2001, MNRAS, 323, 1
- Spergel D.N., et al., 2006, preprint (astro-ph/0603449)
- Springel V., 2005, MNRAS364, 1105
- Springel V., Yoshida N., White S.D.M., 2001, New Astronomy, 6, 79
- Tinker J. L., Norberg P., Weinberg D. H., Warren M. S., 2006, astro-ph/0603543
- Torri E., Meneghetti M., Bartelmann M., Moscardini L., Rasia E., Tormen G., 2004, MNRAS, 349, 476
- van den Bosch F., Mo H. J., Yang X. H., 2003, MNRAS, 345, 923
- van de Marel R. P., Magorrian J., Carlberg, R. G., Yee, H. K. C., Ellingson, E. 2000, AJ, 119, 2039

- Van Waerbeke L., Mellier Y., Pello R., Pen U.L., McCracken H.J., Jain B. 2002, AA, 393, 369
- Viel M., Haehnelt M. G., Lewis A. 2006, astro-ph/0604310
- Voigt L. M., Fabian A. C., 2006, MNRAS, 368, 518
- Wambsganss J., Bode P., Ostriker J. P., 2004, ApJ, 606, L93
- Wittman D., Dell'Antonio I. P., Hughes J. P., Margoniner V. E., Tyson J. A., Cohen J. G., Norman D. 2006, ApJ, 643, 128
- Wu X. P., Hammer F., 1993, MNRAS, 262, 187
- Wu X. P., Mao S., 1996, ApJ, 463, 404
- Yang X. H., Mo H. J., Jing Y. P., van den Bosch F. C., Chu Y. Q., 2004, MNRAS, 350, 1153
- Yang X. H., Mo H. J., van den Bosch F. C., Jing Y. P., 2005, MNRAS, 356, 1293
- Zaritsky D. Gonzalez A. H., 2003, ApJ, 584, 691